Joint International Topical Meeting on Mathematics & Computation and Supercomputing in Nuclear Applications (M&C + SNA 2007)
Monterey, California, April 15-19, 2007, on CD-ROM, American Nuclear Society, LaGrange Park, IL (2007)

USING THE LEVENBERG-MARQUARDT METHOD FOR THE SOLUTION OF INVERSE TRANSPORT PROBLEMS WITH SCATTERING

Keith C. Bledsoe and Jeffrey A. Favorite
Los Alamos National Laboratory
X-4-TAR, MS T082
Los Alamos, New Mexico 87545 USA
kbledsoe@lanl.gov; fave@lanl.gov

ABSTRACT

The Levenberg-Marquardt optimization method is applied to inverse transport problems in a multilayered one-dimensional spherical source/shield system. This method computes a set of unknown parameters using gradients of an error function with respect to each of the unknown parameters. Two problems are considered separately: 1) the unknown parameters are the locations (radii) of material interfaces and 2) the unknown parameters are weight fractions of the constituents of one of the shield materials. The Marquardt method has previously been applied to similar inverse problems in systems which included only unscattered decay gamma-ray lines. Here it is implemented in a system that includes a neutron source surrounded by a material that produces neutron-induced gamma rays. Scattering of both neutrons and photons is accounted for in a 250-energy group structure (130 neutron and 120 photon groups) that includes downscatter, self-scatter, and neutron upscatter. Gradients of the calculated leakages with respect to unknown parameters are calculated using an adjoint-based method. These gradients compare very favorably with gradients calculated using a central-difference approximation. Numerical test cases using two different methods of measurement simulation are considered. Exact radii and material constituents are recovered when measurements are generated using the same spatial and angular discretization as the inverse method. Less accurate results are obtained when more realistic measurements are used.

Key Words: Marquardt method, adjoint-based differentiation, neutron-induced gamma rays

1. INTRODUCTION

The inverse transport problems of determining the location of unknown radii and determining unknown weight fractions of a constituent material in a source/shield system given external leakage measurements have previously been approached by both the Schwinger inverse method [1] and the Levenberg-Marquardt method [2]. In those papers, the methods were successfully applied to inverse transport problems in which only unscattered decay gamma-ray lines were considered.

In this paper, the Levenberg-Marquardt (or simply Marquardt) method is applied to these inverse transport problems in a system with a neutron source and a material that produces neutron-induced gamma rays. As opposed to [1] and [2], scattering of both neutrons and photons is considered here.

The Marquardt method computes a set of unknown parameters using gradients of an error function with respect to each of the unknown parameters. The error function is typically taken to be the χ^2 difference between a set of measured data and a set of model (calculated) data. The data of interest in this paper are the leakages of active gamma lines produced by neutrons in the gamma-inducing material. As was the case in [2], the gradients are calculated using an adjoint-based method [3-5].

In [2], two questions were considered: 1) How well are the gradients calculated using the adjoint-based method and, 2) Given these adjoint-based gradients, how well does the Marquardt method work for these types of problems? These questions will also be addressed in this paper.

2. BACKGROUND

2.1. Notation

Consider a system that includes a volumetric source of neutral particles and some shield. Both the source and shield may be multilayered, but for simplicity only homogeneous layers are considered. The angular flux of both neutrons and photons in the system is given by the Boltzmann transport equation,

$$\hat{\mathbf{\Omega}} \cdot \vec{\nabla} \psi(r, E, \hat{\mathbf{\Omega}}) + \Sigma_t(r, E) \psi(r, E, \hat{\mathbf{\Omega}}) - \int_{4\pi} d\hat{\mathbf{\Omega}}' \int_0^\infty dE' \Sigma_s(r, E' \to E, \hat{\mathbf{\Omega}}' \to \hat{\mathbf{\Omega}}) \psi(r, E', \hat{\mathbf{\Omega}}') = q(r, E, \hat{\mathbf{\Omega}}), \tag{1}$$

where

$\psi(r, E, \hat{\mathbf{\Omega}})$ = angular flux of particles of energy E, position r, and angle $\hat{\mathbf{\Omega}}$

$\Sigma_t(r, E)$ = total cross section at energy E and position r

$\Sigma_s(r, E' \to E, \hat{\mathbf{\Omega}}' \to \hat{\mathbf{\Omega}})$ = scattering cross section at position r from energy E' to E and angle $\hat{\mathbf{\Omega}}'$ to $\hat{\mathbf{\Omega}}$

$q(r, E, \hat{\mathbf{\Omega}})$ = source, at position r, of particles of energy E and angle $\hat{\mathbf{\Omega}}$; units are $\text{cm}^{-3} \cdot \text{s}^{-1}$.

Suppose a set of D measurements is taken at a detector external to the source/shield system. The quantities of interest are

$$M_d = \langle \Sigma_d \psi \rangle, \quad d = 1, \ldots, D, \tag{2}$$

where the inner product notation indicates an integral over all the relevant phase space (volume, angle, and energy). The detector response functions Σ_d are

$$\Sigma_d = \hat{\mathbf{\Omega}} \cdot \hat{\mathbf{n}} \delta(r - r_d), \tag{3}$$

where r_d represents the detector location and $\hat{\mathbf{n}}$ is the outward unit normal at r_d. The response function Σ_d is defined to be zero outside the energy region of interest to detector *d*. In one-dimensional spherical geometry, this definition implies that M_d is the leakage of particles from the source/shield system.

2.2. The Marquardt Method

The Marquardt method was implemented for parameter identification very nearly as described in [6]. Briefly, the method smoothly varies between the inverse-Hessian method and the steepest descent method; a parameter, called λ in [6], is adjusted in each iteration to control the balance. In the present application of the Marquardt method, the error functional to minimize was the standard χ^2:

$$\chi^2 \equiv \sum_{d=1}^{D} \left(\frac{M_{d,\mathrm{o}} - M_d(\mathbf{u})}{\sigma_{d,\mathrm{o}}} \right)^2 , \tag{4}$$

where $M_{d,\mathrm{o}}$ and $\sigma_{d,o}$ are the observed value of the quantity of interest and its associated uncertainty, respectively, and $\mathbf{u} = \{r_n, n = 1,..., N\}$ for the radius identification problem and $\mathbf{u} = \{w_j, j = 1,..., J\}$ for the material composition identification problem.

The equation used to update the *N* unknown radii (or *J* unknown weight fractions) in each iteration is

$$\sum_{l=1}^{N} \alpha'_{kl} \delta u_l = \beta_k, \quad k = 1,...,N, \tag{5}$$

where

$$\beta_k \equiv -\frac{1}{2} \frac{\partial \chi^2}{\partial u_k} \tag{6}$$

and α'_{kl} are slightly modified components of a matrix $\boldsymbol{\alpha}$ whose unmodified components are

$$\alpha_{kl} = \sum_{d=1}^{D} \frac{1}{\sigma_{d,\mathrm{o}}^2} \left(\frac{\partial M_d(\mathbf{u})}{\partial r_k} \frac{\partial M_d(\mathbf{u})}{\partial r_l} \right). \tag{7}$$

The α'_{kl} values are defined in terms of α_{kl} as

$$\alpha'_{kl} \equiv \begin{cases} \alpha_{kl}, & k \neq l \\ \alpha_{kl}(1+\lambda), & k = l. \end{cases} \tag{8}$$

For a weight fraction problem, the terms r_k and r_l in Eq. (7) would be replaced with weight fractions w_k and w_l.

The $\boldsymbol{\alpha}$ matrix of Eq. (7) is actually an approximation of the Hessian matrix that results from ignoring the second derivative terms $\left(1/\sigma_{d,\mathrm{o}}^2\right)\left(M_{d,\mathrm{o}} - M_d(\mathbf{u})\right)\left(\partial^2 M_d(\mathbf{u})/\partial r_k \partial r_l\right)$ that result from differentiating the gradient of χ^2 with respect to the components of $\mathbf{u}$. The $\boldsymbol{\alpha}$ matrix is normally used instead of the Hessian matrix in the Marquardt method [6].

The $\boldsymbol{\alpha}$ matrix may be ill-conditioned, so in this implementation it is inverted using singular value decomposition (SVD) [7], which identifies singular matrices based on a user-specified threshold value. The choice of the threshold can have a large influence on the iteration history for badly conditioned problems. Automatically selecting or adjusting it is a current research topic.

In our implementation of the method for radius identification, when the updated radii end up crossing each other (i.e., $r_n > r_{n+1}$), λ is adjusted until updated radii that are properly ordered are found. This adjustment is initially a reduction in the value of λ by a factor of 10. If the radii again cross, λ is again decreased by a factor of 10. This process repeats until λ has been decreased ten times, after which (if λ still needs readjustment) it is set to 10 times its initial value. If calculated radii continue to cross each other, λ is then repeatedly increased by a factor of 10 until physical radii are found, or for a maximum of 10 times. A similar adjustment of λ occurs for source identification problems if a negative source weight fraction is calculated. Also, if the calculated physical parameters of a given iteration are identical to those of the previous iteration, the problem is reinitialized, with λ returning to its initial value of 0.001.

Implementation of the Marquardt method can be summarized with a brief algorithm [6]:

1. Compute $M_d(\mathbf{u})$ and $\chi^2(\mathbf{u})$ with initially postulated parameters $\mathbf{u}$.
2. Start with $\lambda = 0.001$.
3. Solve Eq. (5) for $\delta\mathbf{u}$. Call the updated parameters $\mathbf{u}' \equiv \mathbf{u} + \delta\mathbf{u}$.
4. If $\mathbf{u}'$ is an unphysical result, modify λ and return to step 3.
5. Calculate $M_d(\mathbf{u}')$ and $\chi^2(\mathbf{u}')$.
6. If $\chi^2(\mathbf{u}') \geq \chi^2(\mathbf{u})$ increase λ by a factor of 10 and go back to step 3.
7. If $\chi^2(\mathbf{u}') < \chi^2(\mathbf{u})$ decrease λ by a factor of 10, update the trial solution, and go back to step 3.

The condition for the algorithm to stop is that the difference between observed and calculated gamma-ray leakages $\left[M_{d,\mathrm{o}} - M_d(\mathbf{u})\right]$ be less than some preset tolerance; in this work, the requirement was that the relative difference be less than 0.01% for each gamma-ray line. The algorithm is also set to stop if the same set of parameters $\mathbf{u}$ are calculated in eight different iterations.

A Fortran code was written to implement the Marquardt method, with a shell script written to control the interfaces between subroutines. The initial (guessed) model is written into an input

file created by the user and read by the code so that calculations could be performed. For subsequent iterations, the code writes a new input file containing the updated parameters **u**.

3. COMPUTING THE GRADIENTS

Consider again the source/shield system described in Sec. 2. If the system is perturbed in some way, the transport equation is given by

$$\begin{aligned}\hat{\mathbf{\Omega}}\cdot\vec{\nabla}\psi'(r,E,\hat{\mathbf{\Omega}})+\Sigma_t'(r,E)\psi'(r,E,\hat{\mathbf{\Omega}})\\ -\int_{4\pi}d\hat{\mathbf{\Omega}}'\int_0^\infty dE'\Sigma_s'(r,E'\to E,\hat{\mathbf{\Omega}}'\to\hat{\mathbf{\Omega}})\psi'(r,E',\hat{\mathbf{\Omega}}')=q'(r,E,\hat{\mathbf{\Omega}}),\end{aligned} \tag{9}$$

where the perturbed cross sections, fluxes, and inhomogeneous source are denoted with a prime. The exact value of the perturbed quantity of interest for detector *d* is

$$M_d'=\left\langle\Sigma_d\psi'\right\rangle, \tag{10}$$

and the variation in the quantity of interest for measurement *d* is

$$\delta M_d=M_d'-M_d=\left\langle\Sigma_d\delta\psi\right\rangle. \tag{11}$$

It is shown in [2] that with the use of the adjoint transport equation,

$$\begin{aligned}-\hat{\mathbf{\Omega}}\cdot\vec{\nabla}\psi_d^*(r,E,\hat{\mathbf{\Omega}})+\Sigma_t(r,E)\psi_d^*(r,E,\hat{\mathbf{\Omega}})\\ -\int_{4\pi}d\hat{\mathbf{\Omega}}'\int_0^\infty dE'\Sigma_s'(r,E\to E',\hat{\mathbf{\Omega}}\to\hat{\mathbf{\Omega}}')\psi_d^*(r,E',\hat{\mathbf{\Omega}}')=\Sigma_d(r,E,\hat{\mathbf{\Omega}}),\end{aligned} \tag{12}$$

the variation in the quantity of interest can be expressed by

$$\delta M_d=\left\langle\psi_d^*,\delta q\right\rangle-\left\langle\psi_d^*,\delta\Sigma_t\psi\right\rangle+\left\langle\psi_d^*,\delta S(r,E,\hat{\mathbf{\Omega}})\right\rangle, \tag{13}$$

where

$$\delta S(r,E,\hat{\mathbf{\Omega}})\equiv\int_{4\pi}d\hat{\mathbf{\Omega}}'\int_0^\infty dE'\delta\Sigma_s(r,E'\to E,\hat{\mathbf{\Omega}}'\to\hat{\mathbf{\Omega}})\psi(r,E',\hat{\mathbf{\Omega}}'). \tag{14}$$

3.1. Unknown Interface Radii

Suppose that in the source/shield system the material compositions are known but the locations of the interfaces between layers are unknown. In such a case, the variations in Eq. (13) are given by

$$\delta\Sigma_t(r,E) = \sum_{n=1}^{N} \delta(r-r_n)\Delta\Sigma_{t,n}(E)\delta r_n\,, \tag{15}$$

$$\delta q(r,E,\hat{\mathbf{\Omega}}) = \sum_{n=1}^{N} \delta(r-r_n)\Delta q_n(E,\hat{\mathbf{\Omega}})\delta r_n\,, \tag{16}$$

and

$$\delta S(r,E,\hat{\mathbf{\Omega}}) = \sum_{n=1}^{N} \delta(r-r_n)\Delta S_n(r,E,\hat{\mathbf{\Omega}})\delta r_n\,, \tag{17}$$

where

$$\Delta\Sigma_{t,n}(E) \equiv \Sigma_{t,n}(E) - \Sigma_{t,n+1}(E)\,, \tag{18}$$

$$\Delta q_n(E,\hat{\mathbf{\Omega}}) \equiv q_n(E,\hat{\mathbf{\Omega}}) - q_{n+1}(E,\hat{\mathbf{\Omega}})\,, \tag{19}$$

$$\Delta S_n(r,E,\hat{\mathbf{\Omega}}) \equiv \int_{4\pi} d\hat{\mathbf{\Omega}}' \int_0^\infty dE' \Delta\Sigma_{s,n}(E'\to E,\hat{\mathbf{\Omega}}'\to\hat{\mathbf{\Omega}})\psi(r,E',\hat{\mathbf{\Omega}}')\,, \tag{20}$$

and

$$\Delta\Sigma_{s,n}(E'\to E,\hat{\mathbf{\Omega}}'\to\hat{\mathbf{\Omega}}) \equiv \Sigma_{s,n}(E'\to E,\hat{\mathbf{\Omega}}'\to\hat{\mathbf{\Omega}}) - \Sigma_{s,n+1}(E'\to E,\hat{\mathbf{\Omega}}'\to\hat{\mathbf{\Omega}})\,. \tag{21}$$

If these expressions are inserted into Eq. (13) and then use is made of the equation [3]

$$\delta M_d = \sum_{i=1}^{I} \frac{\partial M_d}{\partial u_i}\delta u_i\,, \tag{22}$$

the gradient of the quantity of interest with respect to unknown radius n (n = 1,…,N) is

$$\begin{aligned}\frac{\partial M_d}{\partial r_n} = &\int_{4\pi} d\hat{\mathbf{\Omega}} \int_0^\infty dE \psi_d^*(r_n,E,\hat{\mathbf{\Omega}})\Delta q_n(E,\hat{\mathbf{\Omega}}) - \int_{4\pi} d\hat{\mathbf{\Omega}} \int_0^\infty dE \psi_d^*(r_n,E,\hat{\mathbf{\Omega}})\Delta\Sigma_{t,n}(E)\psi(r_n,E,\hat{\mathbf{\Omega}}) \\ &+ \int_{4\pi} d\hat{\mathbf{\Omega}} \int_0^\infty dE \psi_d^*(r_n,E,\hat{\mathbf{\Omega}})\Delta S_n(r_n,E,\hat{\mathbf{\Omega}}).\end{aligned} \tag{23}$$

3.2. Unknown Material Composition

Now suppose the geometry of the source/shield system is known but the weight fractions of the gamma-producing material are unknown. For unknown weight fractions the variations in Eq. (13) are given by

$$\delta\Sigma_{t,s} = \rho_s N_A \sum_{j=1}^{J} \frac{\sigma_{t,j}(E)}{A_j} \delta w_j \tag{24}$$

and

$$\begin{aligned} \delta S &= \delta\Sigma_{s,s}(E' \to E, \hat{\mathbf{\Omega}}' \to \hat{\mathbf{\Omega}}) \\ &= \rho_s N_A \sum_{j=1}^{J} \frac{\sigma_{s,j}(E' \to E, \hat{\mathbf{\Omega}}' \to \hat{\mathbf{\Omega}})}{A_j} \delta w_j , \end{aligned} \tag{25}$$

where the subscript *s* indicates the unknown induced-gamma source region. Here δq is equal to zero because the composition and geometry of the neutron source are known.

Again using Eq. (22), the gradient of the measured leakage with respect to unknown weight fraction *j* (*j* = 1,…,*J*) is given by

$$\frac{\partial M_d}{\partial w_j} = \frac{\rho_S N_A}{A_j} \left[\left\langle \psi_d^*, \int_{4\pi} d\hat{\mathbf{\Omega}}' \int_0^\infty dE' \sigma_{s,j}(E' \to E, \hat{\mathbf{\Omega}}' \to \hat{\mathbf{\Omega}}) \psi(r, E', \hat{\mathbf{\Omega}}') \right\rangle_s - \left\langle \psi_d^*, \sigma_{t,j} \psi \right\rangle_s \right]. \tag{26}$$

4. COMPARISON OF NUMERICAL DERIVATIVES

The adjoint-based derivatives of Eqs. (23) and (26) were compared to derivatives calculated using a central difference approximation. Forward and adjoint fluxes were calculated using the multigroup discrete-ordinates code PARTISN [8] with S_{32} quadrature and P_3 scattering. The ACTI library, a multigroup cross section library for (n, γ) applications developed at Los Alamos National Laboratory, was used in the calculations [9]. The ACTI library has 130 neutron groups (52 of which include upscattering) and 120 photon groups.

4.1. Unknown Radii

For the case of unknown radii, a one-dimensional spherical model, similar to that used in [10], was used for comparison of derivatives. The model consisted of a neutron source of radius 4.0 cm consisting of aluminum impregnated with californium-252; this source was modeled as pure aluminum with mass density 2.7 g/cm^3. This source was surrounded by a shell of a single homogeneous material composed of carbon, hydrogen, nitrogen, and oxygen with weight fractions 0.3112, 0.0279, 0.2934 and 0.3675, respectively. This CHNO material had a mass density of 1.678 g/cm^3 and inner and outer radii of 5.0 and 12.0 cm. Outside the CHNO shield was a region of void with a radius of 20.0 cm. The quantities of interest were the leakages of gamma lines induced in CHNO due to interaction with neutrons emitted from the Cf-252 source. The active lines considered were the 1.8848-MeV nitrogen line, 2.2246-MeV hydrogen line, and the 3.684- and 4.9464-MeV carbon lines. This model will be referred to as the CHNO model.

Central difference results were obtained by varying each interface by ± 0.0001 cm independently. Tables I, II, and III illustrate that central difference and adjoint-based derivatives

differ by 0.5% or less for each energy line for all three radii, with the exception of a 3.71% relative error for the 3.684 MeV line for the 5.0 cm radius.

The accuracy of the adjoint-based derivatives for this problem, which includes neutron and gamma-ray scattering, is similar to that found in [2] for a similar geometry using only unscattered decay gamma rays. This is a reassuring result, since it was thought that adding the scattering term would decrease the accuracy of the adjoint-based derivatives. (It should be noted that, in [2], the most inaccurate derivatives were those calculated for the gamma-ray source. A similar comparison here would look at the derivatives of neutron leakage with respect to the neutron source radius, which was not done.)

Table I. Comparison of Central Difference and Adjoint Based Derivatives for r = 4.0 cm (Neutron Source)

Active Line (MeV)	$\frac{\partial M_d}{\partial r}$ (Cent Diff)	$\frac{\partial M_d}{\partial r}$ (Adjoint)	Relative Difference (%)
1.8848	236.0	235.7	–0.13
2.2246	7725	7717	–0.10
3.6840	1005	1008	0.30
4.9464	27.35	27.34	–0.04

Table II. Comparison of Central Difference and Adjoint Based Derivatives for r = 5.0 cm

Active Line (MeV)	$\frac{\partial M_d}{\partial r}$ (Cent Diff)	$\frac{\partial M_d}{\partial r}$ (Adjoint)	Relative Difference (%)
1.8848	–82.50	–82.60	0.12
2.2246	–2735	–2733	–0.07
3.6840	–105.0	–108.9	3.71
4.9464	–9.85	–9.87	0.20

Table III. Comparison of Central Difference and Adjoint-Based Derivatives for r = 12.0 cm

Active Line (MeV)	$\frac{\partial M_d}{\partial r}$ (Cent Diff)	$\frac{\partial M_d}{\partial r}$ (Adjoint)	Relative Difference (%)
1.8848	100.0	100.2	0.20
2.2246	3330	3325	–0.15
3.6840	85.00	85.35	0.41
4.9464	12.10	12.09	-0.08

4.2. Unknown Weight Fractions

For unknown weight fractions, comparison between adjoint-based and central difference derivatives was accomplished using a model with the same geometry and neutron source as the CHNO model, but the single shield layer contained only two isotopes. Since weight fractions cannot be varied independently, the full derivative of the quantity of interest with respect to the weight fraction of the first isotope is

$$\begin{aligned}\frac{dM_d}{dw_1} &= \frac{\partial M_d}{\partial w_1} + \frac{\partial M_d}{\partial w_2}\frac{dw_2}{dw_1} \\ &= \frac{\partial M_d}{\partial w_1} - \frac{\partial M_d}{\partial w_2},\end{aligned} \tag{27}$$

while the full derivative with respect to the second isotope is

$$\begin{aligned}\frac{dM_d}{dw_2} &= \frac{\partial M_d}{\partial w_2} + \frac{\partial M_d}{\partial w_1}\frac{dw_1}{dw_2} \\ &= -\frac{dM_d}{dw_1}.\end{aligned} \tag{28}$$

The second lines of Eqs. (27) and (28) obtain because $w_1 + w_2 = 1$.

The partial derivatives on the right side of Eq. (27) were calculated using the adjoint-based method, while the full derivatives on the left side were calculated using a central difference. The unknown isotopes were carbon and hydrogen, each at 50%. A comparison of the two sides of Eq. (27) (where w_1 is the weight fraction of carbon and w_2 the weight fraction of hydrogen) is presented in Table IV. (Since nitrogen is not present in the gamma-emitting material, the 1.8848-MeV line is not used in this comparison.) Table IV illustrates that the difference between the two methods of differentiation is less than 2% for each energy line.

Table IV. Comparison of the Left and Right Sides of Eq. (27) for a Material Containing Carbon and Nitrogen at 50%

Active Line (MeV)	Left Side of Eq. (27)	Right Side of Eq. (27)			Relative Difference Between Left and Right Side (%)
	$\frac{dM_d}{dw_{carbon}}$ (Cent. Diff)	$\frac{\partial M_d}{\partial w_{carbon}}$	$\frac{\partial M_d}{\partial w_{nitrogen}}$	$\frac{dM_d}{dw_{carbon}}$ (Adjoint)	
2.2246	160000	–149500	–312200	162700	1.69%
3.6840	2170	802	–1410	2212	1.94%
4.9465	375.5	128.1	–248.3	376.4	0.24%

5. TEST PROBLEMS

For the numerical test problems, the observed values $M_{d,o}$ used in χ^2 of Eq. (4) were simulated in two different ways. The first method used PARTISN to calculate measurements with the known true configuration using the same spatial and angular discretization as used in the Marquardt method transport calculations. Uncertainties for this case were arbitrarily set to 1%. Since PARTISN was used with S_{32} angular discretization to produce these values, this set of measurements will be referred to as S_{32} measurements. The second method used the Monte Carlo code MCNP [11] to generate less consistent, more realistic measurements. This set of measurements will be referred to as Monte Carlo measurements. Table V gives the results of the simulation for each measurement method. The CHNO model of Sec. 4.1 was used for both unknown radius and unknown weight fraction test problems.

Table V. Simulated Leakage Measurements (γ/s) with S_{32} and Monte Carlo Methods

Active Line (MeV)	S_{32} Measurement	Monte Carlo Measurement
1.8848	3.05349E+02	3.36000E+02 ± 5.45%
2.2246	9.99297E+03	1.02900E+04 ± 1.02%
3.6840	1.41914E+03	1.45800E+03 ± 2.65%
4.9465	3.53495E+01	4.60000E+01 ± 14.74%

5.1 Determination of Unknown Radii

Two test problems are presented to illustrate identification of unknown radii. In the first, the radius of the neutron source was known but the inner and outer radii of the CHNO shield were unknown. In the second, the source radius and the shield radii were all unknown.

5.1.1 Test Problem 1: Determination of Inner and Outer Shield Radii, Known Source Radius

The radius of the neutron source was known to be 4.0 cm, but the shield radii were unknown, with the initial guess for the inner and outer radii being 7.0 cm and 10.0 cm, respectively. When S_{32} measurements were used, the method converged exactly to the correct radii, 5.0 cm and 12.0 cm, in six iterations.

When Monte Carlo measurements were used, the inner and outer radio of the CHNO shield were calculated in the first iteration to be 32.4 cm and 40.0 cm. Since the outer boundary of the void layer that surrounds the geometry is at 20.0 cm, this was an unphysical result. Thus λ was adjusted from its initial value of 0.001 to 0.0001 (step 4 of the Marquardt algorithm) and the unknown radii were again calculated. However, with $\lambda = 0.0001$ the inner and outer radii of the shield were calculated to be 54.5 and 63.2 cm, results that were again unphysical. This process of adjusting λ yet finding unphysical results continued until λ had been decreased ten times to 1.0E–12. Thus λ was next adjusted back to its initial value of 0.001 times 10. With this value unphysical radii were calculated yet again, and λ was increased by a factor of ten to 0.1. With $\lambda = 0.1$ realistic shield radii of 8.61 and 19.3 cm were finally calculated, and the iterative process

could continue. In the second iteration, with λ still equal to 0.1, the inner layer of the CHNO shield was calculated to be 3.82 cm, an unphysical result because the radius of the neutron source was 4.0 cm. Thus λ was decreased by a factor of 10 to 0.01. With this value the calculated CHNO radii were again calculated to be 8.61 and 19.3 cm, seemingly identical to the results in the previous iteration. Closer inspection, however, revealed that in the second iteration the radii were calculated to be 8.60976617 and 19.1340440 and in the third iteration they were 8.60976628 and 19.1340441. These very slight differences meant that there was not a repeat in results and thus the problem did not reinitialize. Instead, $\chi^2(\mathbf{u}') \geq \chi^2(\mathbf{u})$ and λ was increased by a factor of 10 to 0.1 (step 6 in the Marquardt algorithm of Sec. 2.2). In the fourth iteration, nearly the same phenomenon was seen: λ was initially 0.1 but an unphysical radius was calculated, resulting in λ being adjusted to 0.01. With that value of λ, CHNO radii were calculated that were nearly but not exactly identical to those in the previous generation. This pattern repeated indefinitely, resulting in a failure of the method.

Two solutions to this problem are possible. First, the calculation can be restarted using the almost-repeated radii of 8.61 cm and 19.3 cm as the initially guessed radii. A newly initialized calculation leads to a successful result. The second solution is to reduce the number of digits used by the Fortran code to represent the calculated radii. While very high accuracy is needed when S_{32} measurements are used, this is not the case for Monte Carlo measurements. If only four-digit accuracy were used with the Monte Carlo measurements, for instance, the calculated radii in the second and third iterations would have been 8.6097and 19.1340, identical results that would have lead to a reinitialization and a successful conclusion to the problem.

After either of these solutions were tried, χ^2 dropped to a value of 3.315 in six iterations, at which point solutions began repeating. For this value of χ^2 the calculated shield radii were 4.26 and 11.50, which have relative differences of 14.80% and 4.17%, respectively, from the actual radii of 5.0 and 12.0 cm. These results summarized in Table VI. The iteration history (χ^2 vs. iteration number) for both S_{32} and Monte Carlo measurements for this problem is shown in Fig. 1.

Table VI. Results for Test Problem 1

Measurement Method	Actual Radius (cm)	Calculated Radius (cm)	% Difference
S_{32}	5.00	5.00	0.00
	12.00	12.00	0.00
Monte Carlo	5.00	4.26	14.80
	12.00	11.50	4.17

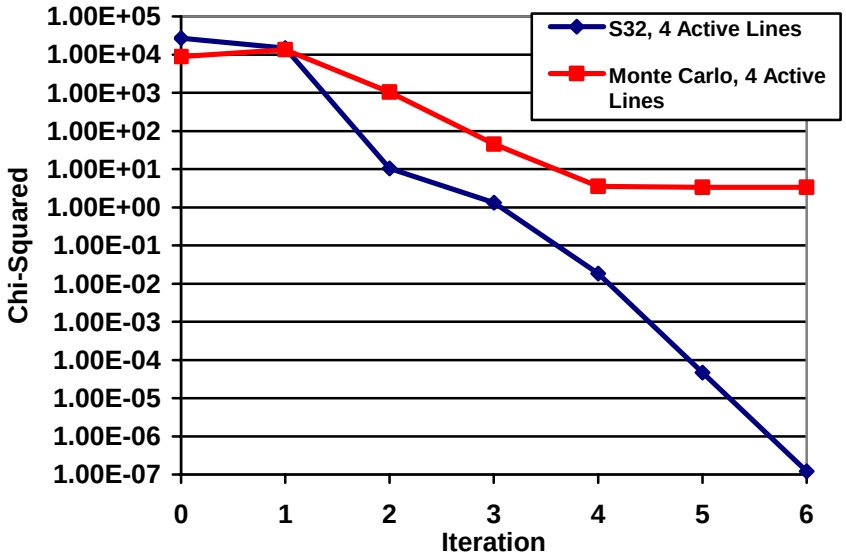

Figure 1: Convergence for Test Problem 1.

Test Problem 2: Determination of Source Radius and Inner and Outer Shield Radii

The second test problem for determining unknown radii featured not only unknown inner and outer radii of the CHNO shield, but also an unknown neutron source radius. The initial guess for the three radii was 3.0, 7.0, and 10.0 cm. Figure 2 illustrates the iteration history for both sets of measurements. With S_{32} measurements the method converged to the exact radii (4.00, 5.00, 12.00) in ten iterations. When Monte Carlo measurements were used, χ^2 dropped to 3.32 after ten iterations, at which point results began repeating. For this value of χ^2, radii of 4.03, 4.80, and 11.90 were calculated. These values have relative differences of 0.75%, –4.00%. and 0.83%, respectively, from the actual radii. The results for this problem are summarized in Table VII.

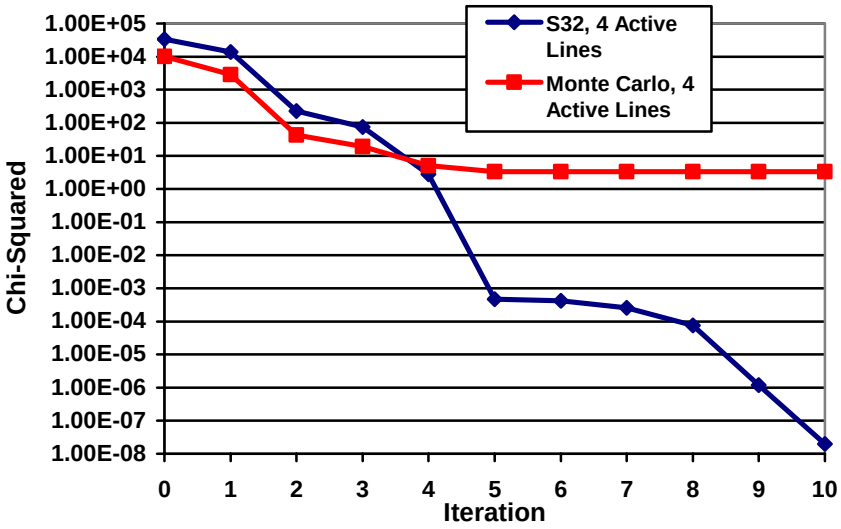

Figure 2: Convergence for Test Problem 2.

Table VII. Results for Test Problem 2

Measurement Method	Actual Radius (cm)	Calculated Radius (cm)	% Difference
S_{32}	4.00	4.00	0.00
	5.00	5.00	0.00
	12.00	12.00	0.00
Monte Carlo	4.00	4.03	0.75
	5.00	4.80	–4.00
	12.00	11.90	0.83

5.1 Test Problem 3: Determination of Unknown Weight Fractions

The method for determining unknown weight fractions in the gamma-producing material was tested on a problem in which the weight fractions of all four constituents of the CHNO layer were unknown. An initial guess of 0.2500 was made for all four of the isotopes. The iteration history for this problem is presented in Fig. 3. When S_{32} measurements were used, the method converged to the correct weight fractions (carbon: 0.3112, hydrogen: 0.0279, nitrogen: 0.2934, and oxygen: 0.3675) in 12 iterations. With Monte Carlo measurements χ^2 dropped to 2420 after 19 iterations, and results began repeating. The weight fractions corresponding to this value of χ^2 and differences between these values and the actual CHNO weight fractions are shown in Table VIII. While relative differences are larger than were found in radius identification problems, the method did successfully identify the correct order of the weight fractions.

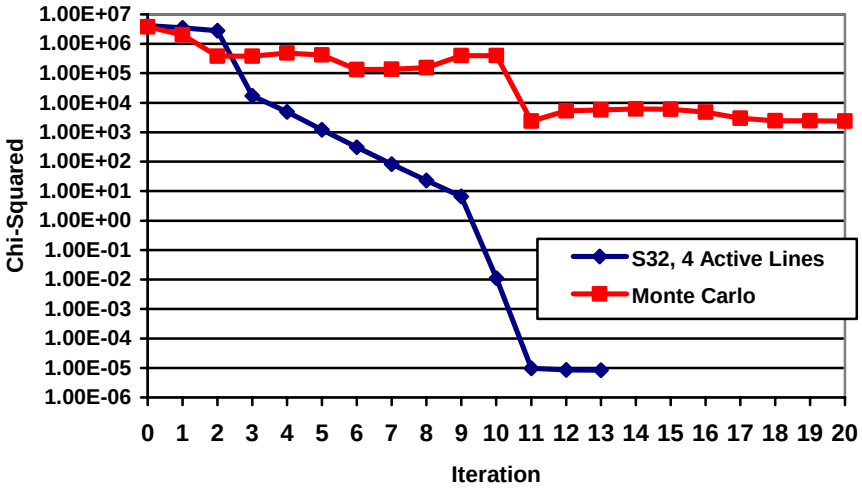

Figure 3: Convergence for Test Problem 3.

Table VIII. Results for Test Problem 3

Measurement Method	Isotope	Actual Weight Fraction	Calculated Weight Fraction	% Difference
S_{32}	Carbon	0.3112	0.3112	0.00
	Hydrogen	0.0279	0.0279	0.00
	Nitrogen	0.2934	0.2934	0.00
	Oxygen	0.3675	0.3675	0.00
Monte Carlo	Carbon	0.3112	0.2357	–24.3
	Hydrogen	0.0279	0.0212	–24.0
	Nitrogen	0.2934	0.1365	–53.5
	Oxygen	0.3675	0.6066	65.1

6. CONCLUSIONS

The Marquardt method has been implemented in a system in which neutron and photon scattering are considered. Using neutron-induced gamma lines, unknown interface radii and unknown weight fractions were (separately) identified in a material containing carbon, hydrogen, nitrogen, and oxygen. The necessary gradients, which were computed using an adjoint-based method, were compared with central difference results. These comparisons were very favorable for both radii and weight fractions, and the adjoint-based gradients were used for successful reconstruction of the unknown system.

Numerical test problems for radius and source identification were implemented using two different methods for simulating leakage measurements. In the first method, the leakages were generated using the same spatial and angular discretization as used in the iterative calculations, resulting in leakage values exactly consistent with calculated results. With these measurements, the exact values of the unknown radii and weight fractions were always found. The second set of measurements were generated by MCNP, resulting in less accurate (and thus more realistic) values. When these leakages were used, the method found results within 5% for unknown radius problems, but had errors of between 20% and 70% for unknown weight fractions.

REFERENCES

1. J. A. FAVORITE, "Using the Schwinger Variational Functional for the Solution of Inverse Transport Problems," *Nucl. Sci. Eng.*, **146**, 51-70 (2004).
2. J. A. FAVORITE and D. I. KETCHESON, "Using the Levenberg-Marquardt Method for the Solution of Inverse Transport Problems," *Trans. Am. Nucl. Soc.*, **95**, 527-531 (2006).
3. S. J. NORTON, "A General Nonlinear Inverse Transport Algorithm Using Forward and Adjoint Flux Computations," *IEEE Trans. Nucl. Sci.*, **44**, 153-162 (1997).
4. J. A. FAVORITE and R. SANCHEZ, "An Inverse Method for Radiation Transport," 10th International Conference on Radiation Shielding/Radiation Protection and Shielding 2004, Funchal, Portugal, May 9-14; *Radiation Protection Dosimetry,* **116**, *1-4*, 482-485 (2005).

5. J. C. RAGUSA, "Application of Duality Principles to Solve Inverse Particle Transport Problems: A Framework," *Trans*. *Am*. *Nucl*. *Soc*., **93**, 427-429 (2005).
6. W.H. PRESS et al., *Numerical Recipes in FORTRAN: The Art of Scientific Computing*, 2nd Ed. (reprinted with corrections), Chap. 15, Cambridge University Press (1994).
7. W.H. PRESS et al., *Numerical Recipes in FORTRAN: The Art of Scientific Computing*, 2nd Ed. (reprinted with corrections), Chap. 2, Cambridge University Press (1994).
8. R. E. ALCOUFFE et al., "PARTISN," LA-CC-98-62, Los Alamos National Laboratory (1997).
9. S. FRANKLE, "A Prototype Fine-Group Library for Gamma-Ray Spectroscopy, ACTI," Internal Memorandum XCI:SCF-99-19(U), Los Alamos National Laboratory (2004).
10. J. A. FAVORITE, "Variational Estimates of Neutron-Induced Gamma Line Leakages and Ratios for Internal Interface Perturbations," *Nucl. Sci. Eng.*, **155**, 321-329 (2007).
11. X-5 Monte Carlo Team, "MCNP-A General Monte Carlo N-Particle Transport Code, Version 5," Vol. I, LA-UR-03-1987, Los Alamos National Laboratory (2003).